TOPLHA: an accurate and efficient numerical tool for analysis and design of LH antennas

Terms of use:

Publisher copyright

(Article begins on next page)

16 June 2025

TOPLHA: an Accurate and Efficient Numerical Tool for Analysis and Design of LH Antennas

D. Milanesio[1]§, O. Meneghini[2], R. Maggiora[1], S. Guadamuz[1], J. Hillairet[3], V. Lancellotti[4], G. Vecchi[1]

[1] Politecnico di Torino, Dipartimento di Elettronica, Torino, Italy
[2] with Politecnico di Torino at the time of performing this work; now with Massachusetts Institute of Technology, Plasma Science and Fusion Center, Cambdrige, USA
[3] CEA, IRFM, F-13108 Saint Paul-lez-Durance, France
[4] with Politecnico di Torino at the time of performing this work; now with Faculty of Electrical Engineering, Technical University of Eindhoven, The Netherlands

Abstract. This paper presents a self-consistent, integral-equation approach for the analysis of plasma-facing Lower-Hybrid launchers; the geometry of the waveguide grill structure can be completely arbitrary, including non-planar mouth of the grill. The present work is based on the theoretical approach and code implementation of the TOPICA code, of which it shares the modular structure and constitutes the extension into the LH range. Code results are validated against literature results and simulations from similar codes.

§ Author to whom any correspondence should be addressed

1. Motivation and background

Radio-frequency (RF) heating and current drive schemes are used in many existing nuclear fusion *tokamak* devices and they are expected to play a fundamental role in the future reactor scale experiments; for instance, in ITER, Lower Hybrid and Current Drive (LHCD) is foreseen to sustain the steady state phase [1]. Unfortunately, due to the impossibility to fully test the antennas employed in such heating and current drive schemes before the starting of the operations, advanced numerical simulation tools are necessary to efficiently carry out their design.

This consideration first motivated the development of the TOPICA code [2] for Ion Cyclotron (IC) antennas and its extension to a more general multi-cavity approach [3]. In recent years, the TOPICA code has been systematically adopted for the analysis of present IC antennas (see [4]) and the design of future ones (see [5], [6] and [7]). Driven by the same objectives, this paper describes the formulation and validation of a substantial extension of TOPICA to allow for the analysis of Lower Hybrid (LH) antennas: the resulting code will be henceforth referred to as TOPLHA (TOrino Politecnico Lower Hybrid Antennas) code (first presented in [8]).

TOPLHA is based on the same general approach as the IC version TOPICA, but the simulation of LH launchers requires significant modification of the source description (termed port embedding and de-embedding in [3]), since LH antennas are waveguide-fed, while IC antennas are fed by coaxial lines. Even if LH antennas have rather simple geometries with respect to IC antenna systems, their overall electrical size is intrinsically large because of the higher operational frequency. Consequently, a significantly larger number of unknowns, is required to discretize the resulting boundary-value problem. In order to avoid intractable numerical problems, it is therefore essential to suitably exploit the intrinsic multiple-cavity nature of LH antenna geometries, as can be efficiently done adopting the formulation outlined in [3]. We further remark that exploitation of the multi-cavity nature of the LH problem in TOPLHA via [3] lends itself to an efficient parallelization of the code.

Similar codes devoted to the analysis of LH antennas have also been developed, namely ALOHA (Advanced LOwer Hybrid Antenna) [9] and GRILL3D [10]. Their main limitation resides on the antenna side of the problem: while TOPLHA has no constrains in terms of geometrical complexity (any detail of the structure can be included in the simulation process), both ALOHA and GRILL3D can simulate only launchers composed of flat arrays of rectangular waveguides . Conversely, it has to be noted that this limitation, together with the different formulation itself, reflects in shorter run times with respect to TOPLHA.

Recently, finite element methods have been used for LH wave propagation on the plasma core and, to some extent, also for antenna coupling calculations in the LH and IC frequency regimes [11]. The finite element method inherently allows an arbitrary description of both the antenna and the plasma geometry (both in 2D and 3D); a cold plasma is assumed right in front of the launcher, with an absorbing layer to impose the

correct radiating conditions.

For the sake of conciseness, only a short summary of the main background formulation will be given (Sec. 2.1); instead, this paper details the derivation of the new source term (Sec. 2.2) and provides validation examples in vacuum (Sec. 3.1) and with plasma (Sec. 3.2).

2. Formulation

2.1. Background

The TOPLHA code is based on the same formulation of the TOPICA code and, as its progenitor, it is structured to efficiently tackle the complexities arising both from the geometrical structure of LH antennas and from the plasma loading. The interested reader will find in [3] the detailed analysis of the theoretical basis common to TOPICA and TOPLHA. However, for ease of understanding of the present work, we sketch here the main characteristics of the background formulation of TOPLHA. The related boundary-value problem is cast into an integral-equation formulation for the self-consistent evaluation of the current distribution on the antenna conductors. Thanks to the specific adopted formulation, it is possible to seamlessly connect a 3D description of the antenna conductors and a 1D description of the plasma (see [2], appendix A, for details). In it, the environment is subdivided in two self-consistently coupled region, the plasma region and the vacuum region, linked by means of electromagnetic field on the interface between them (termed as "aperture" in [2] and [3]). In the vacuum region all the calculations are executed in the spatial (i.e. natural) domain, while in the plasma region calculations are performed in the spectral (i.e. Fourier-transform) domain.

The plasma enters the formalism via a surface impedance matrix, here generated by means of a suitably modified version of the FELHS code [12] (Finite Element Lower Hybrid Solver). FELHS, as its predecessor for the IC range of frequencies FELICE [13], solves the full wave equation in slab geometry, i.e. computes the plasma surface impedance (a rank-2 tensor linking the tangential components of electric and magnetic fields at the plasma interface) of a 1D inhomogeneous plasma. The most important change is in the codified wave equation, which takes into account a full hot parallel dispersion. This 1D plasma model is then coupled to the full 3D antenna description by means of a convenient geometrical *stretching*, as depicted in Figure 1 and fully detailed in appendix A of [2].

2.2. Port embedding and de-embedding formulation

In [3], we introduced a different perspective to link the antenna input parameters to the forcing terms and the unknowns of the Integral equations (IEs) involved in the problem, essentially based on the fact that coaxial lines are well-defined guiding structures. Moreover, we explicitly reported the equation that relates the input admittance to the modal current for a quite general case of an IC antenna with multiple cavities and multiple ports per cavity.

This alternative approach has been pursued also for the implementation of the LH source term, substituting coaxial cables with rectangular waveguides, but again making use of an 'embedding' and 'de-embedding' procedure. To shortly summarize, we will attain to the same two dual steps: 1) enforce a field boundary condition at the port surface S_P, i.e. linking the forcing term to the port; 2) obtaining the desired antenna
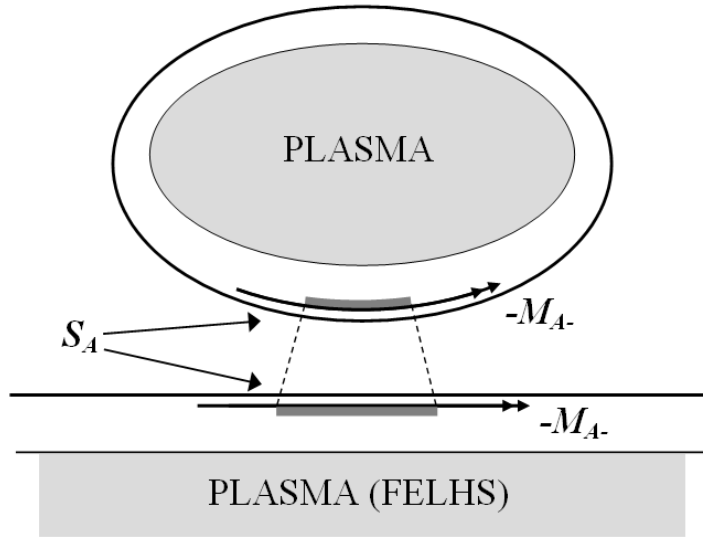
Figure 1. Qualitative representation of the *stretching* procedure described in [2]: the magnetic current surface density $\boldsymbol{M}_{A-}$ is mapped from the surface S_A, which is curved, onto a plane in order to apply the slab plasma approximation.

input parameters from the computed fields at the port surface S_P.

We further observe that we will not necessarily be satisfied with impedance (or admittance) parameters, since the most natural parameterization for waveguides is in terms of scattering parameters; while these can be in principle obtained from the corresponding impedance parameters, it is both computationally and theoretically desirable to derive them directly from the solution of the IEs. In a transmission line, enforcing a boundary condition on a forward wave - as opposed to a voltage or current - requires enforcing a linear combination of voltage and current; likewise, the scattering parameter equivalent to an impedance is the reflection coefficient, that in turn derives from the ratio between forward and backward waves, i.e. from the ratio between two dual linear combinations of voltages and currents.

Even though LH launchers are usually complex grids of waveguides, i.e. multiple cavity devices, in order to ease the understanding of the procedure and to avoid a clumsy notation we limit our detailed derivation to the case of a single waveguide, like the one sketched in Figure 2, and single-mode operation; in these conditions the general S-matrix reduces to the reflection coefficient for the considered waveguide mode. Extension to multiple ports and multi-mode operation is straightforward, and summarized at the end of the section.

The relation between the (modal) travelling wave amplitudes V_P^+, $V_P^- = V_P^+\Gamma$ and the fields is expressed by

$$\boldsymbol{E}_P = V_P^+(1+\Gamma)\boldsymbol{e} \tag{1}$$

$$\boldsymbol{H}_P = \frac{1}{Z_P}V_P^+(1-\Gamma)(\hat{\boldsymbol{n}} \times \boldsymbol{e}) \ , \tag{2}$$

where Γ is the unknown reflection coefficient, $\boldsymbol{e}$ is the (electric) modal eigenfunction, Z_P
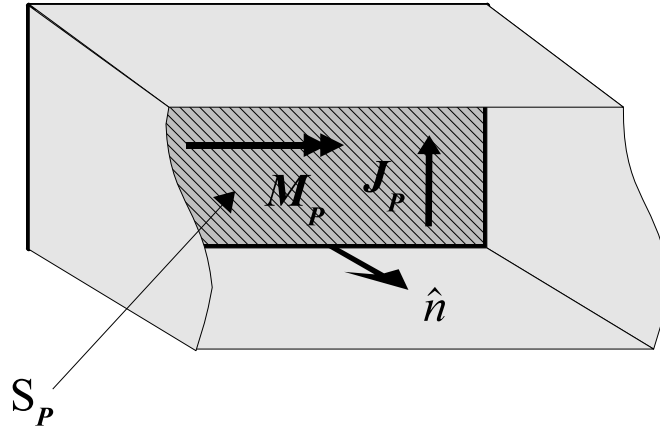
Figure 2. Electric and magnetic equivalent current densities are defined over the waveguide port aperture.

is the (known) characteristic impedance of the considered mode ([15],[16]), and where all modal indices have been omitted for the economy of notation. We observe that the choice of the modal impedances for waveguide modes is largely arbitrary, but it must be consistent with the choice of the normalization of the modal eigenfunctions; in the following, we have assumed the choice adopted in [15].

We notice that the electric and magnetic fields are further related to the magnetic and electric equivalent currents via

$$\boldsymbol{M}_P = \boldsymbol{E}_P \times \hat{\boldsymbol{n}}, \quad \boldsymbol{J}_P = \hat{\boldsymbol{n}} \times \boldsymbol{H}_P, \tag{3}$$

wherein $\hat{\boldsymbol{n}}$ is the unit vector normal to S_P and pointing inwards the waveguide, and $\boldsymbol{E}_P$, $\boldsymbol{H}_P$ are the unknown fields on S_P. We could then choose any one of the two equations (1) (2) above as the one to be enforced. However, differently from the admittance case, the above relationships involve both fields and the final unknown (Γ); before choosing one of the fields as unknown and the other as the one to be enforced, we need therefore to clarify the role of the final unknown, the reflection coefficient. Summing and subtracting (1) and (2), one can eliminate Γ or make it explicit:

$$\frac{1}{2}(\boldsymbol{E}_P + Z_P \boldsymbol{H}_P \times \hat{\boldsymbol{n}}) = V_P^+ \boldsymbol{e} \tag{4}$$

$$\frac{1}{2}(\boldsymbol{E}_P - Z_P \boldsymbol{H}_P \times \hat{\boldsymbol{n}}) = V_P^+ \Gamma \boldsymbol{e} \tag{5}$$

The first equation, (4), does not contain the unknown term Γ, and can therefore be retained as the field boundary condition to be enforced in the IEs; we recall that the fields are further related to the equivalent currents on the port aperture, and we choose to keep as unknown the electric current $\boldsymbol{J}_P$ (i.e. the magnetic field). Equation (4) will therefore constitute the port embedding boundary equation,

$$\frac{1}{2}(\boldsymbol{E}_P - Z_P \boldsymbol{J}_P) = V_P^+ \boldsymbol{e} \tag{6}$$

Observe that $\boldsymbol{E}_P$ is due to the radiation of the currents on the port ($\boldsymbol{J}_P$) and everywhere else ($\boldsymbol{J}_c$), so that the above is in fact an integral equation that will have to be added to the IEs described in [3] (Section 2) and tested in the Method of Moments (MoM) discretization procedure (see [2]). At a difference with the admittance case, the above relationships contains both the known term ($V_P^+\boldsymbol{e}$) and the unknown function $\boldsymbol{J}_P$; in the resulting MoM linear system, it will therefore contribute to both the LHS and the RHS. Using the same notation used above, we can recast (6) so as to stress its role as an IE:

$$\frac{1}{2}\chi_P(\boldsymbol{E}_P[\boldsymbol{J}_P, \boldsymbol{J}_c] - Z_P\boldsymbol{J}_P) = \chi_P V_P^+\boldsymbol{e} \tag{7}$$

where χ_P is the characteristic Kroneker function of the port aperture S_P (i.e. it is defined as one on it and zero everywhere else).

The second equation, (5), contains the unknown input parameter, and will be used to gather it after the associated fields combination has been determined by the numerical solution. This is obtained via projection of (5) onto the set of the waveguide modes; recalling the orthonormality property of this set, one readily arrives at

$$2V_P^+\Gamma = \langle\boldsymbol{e}, \boldsymbol{E}_P\rangle - Z_P\langle\boldsymbol{e}, \boldsymbol{H}_P \times \hat{\boldsymbol{n}}\rangle \tag{8}$$

Having chosen to keep $\boldsymbol{J}_P$ as unknown, this yields

$$\Gamma = \frac{Z_P}{V_P^+}\langle\boldsymbol{e}, \boldsymbol{J}_P\rangle + 1 \tag{9}$$

where we have used the equivalence between electric current and magnetic field defined in (3). Notice that (9) is an explicit expression for the final unknown Γ in terms of the IE unknown $\boldsymbol{J}_P$, i.e. the de-embedding equation.

Equation (9) can be straightforwardly generalized in case of an entire LH launcher made up of several waveguides, each of them being a port. If one wishes to consider multi-mode operation, or one is interested in multi-mode characterization of the discontinuity, then it is necessary to consider the additional modes as ports of the equivalent network. E.g., if we consider a pair of physical waveguide ports, and we want to account for three modes on each waveguide, the equivalent network will have six ports.

The results for the general case are listed next without derivation. A specific element of the scattering matrix can be determined as:

$$S_{ls} = \frac{\sqrt{Y_l}V_l^-}{\sqrt{Y_s}V_s^+} = \frac{\sqrt{Y_l}(V_l^+ + Z_l\langle\boldsymbol{e}_l, \boldsymbol{J}_l\rangle)}{\sqrt{Y_s}V_s^+} \tag{10}$$

i.e. by driving port s with an incident wave of voltage V_s^+ and measuring the reflected wave amplitude V_l^- coming out of port l, being the incident wave in all other ports equal to zero. Moreover, Y_l is the reference admittance at port l, while Y_s is the reference admittance at port s.

3. Code validation

3.1. Waveguides in vacuum

As a very first validation of the TOPLHA code, a rather simple antenna has been analyzed, namely a rectangular waveguide radiating off a perfectly conducting flange of infinite extent, in free space. The commercial electromagnetic simulation software *CST-Microwave Studio*‡ (MWS) has been used as an independent reference: in addition to being one of the most widespread commercial tools in this community, it is important to remark that MWS is based on a completely different numerical approach, thus standing as an independent comparison.

The ratio between sides a and b of the waveguides has been fixed to 2.25 (i.e. $a = 4.5$cm and $b = 2$cm); while Figure 3 shows the problem geometry simulated in TOPLHA (an infinite ground plane is assumed to be located at the waveguide mouth), a waveguide with a finite flange has been simulated (see Figure 4) with *CST-Microwave Studio*.
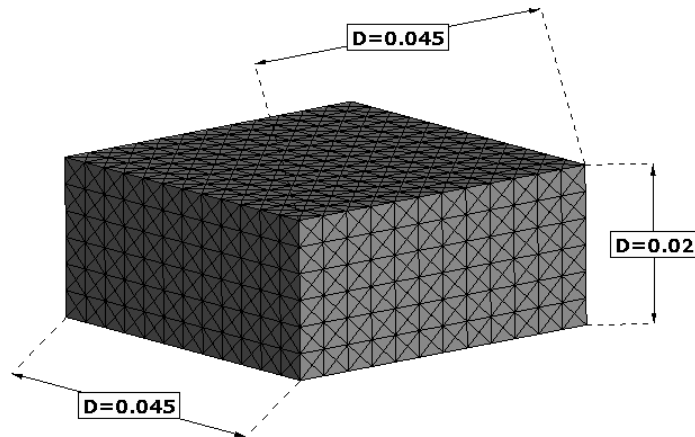
Figure 3. Rectangular waveguide simulated with TOPLHA code with its relevant dimensions and the adopted triangular mesh.

The results computed by TOPLHA and *CST-Microwave Studio* are plotted in magnitude and phase in Figure 5 and 6 respectively.

As can be seen, the two codes compare pretty well in both magnitude and phase along the shown frequency range. The small differences seen in the figures are essentially concentrated in the resonance-like region around the waveguide TE_{10} cutoff frequency ($f_c = 3.33$GHz); they can be ascribed to the finite vs. infinite size of the ground plane, and are inessential (the precise value of the matching at cutoff transition is well-known to be very dependent on parameters like the size of finite ground plane, and practically irrelevant [14]).
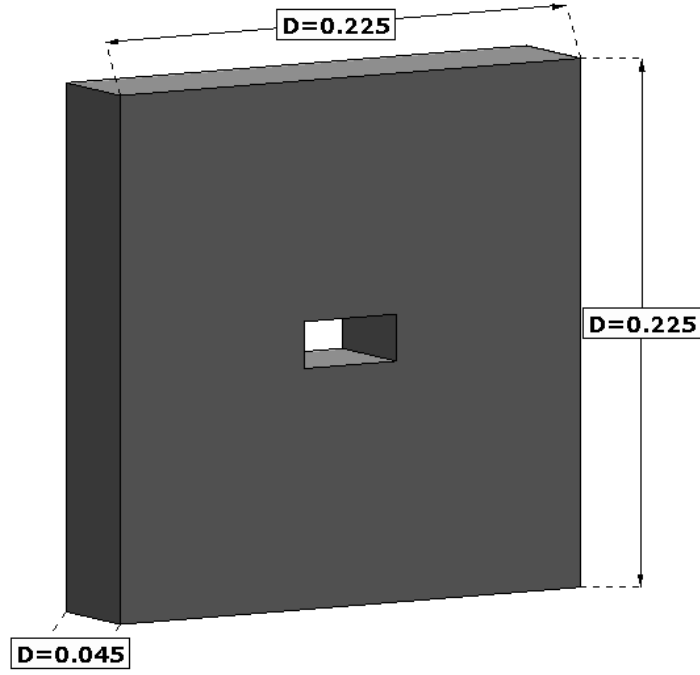
‡ www.cst.com

Figure 4. Rectangular waveguide simulated with MWS-CTS code with its relevant dimensions.
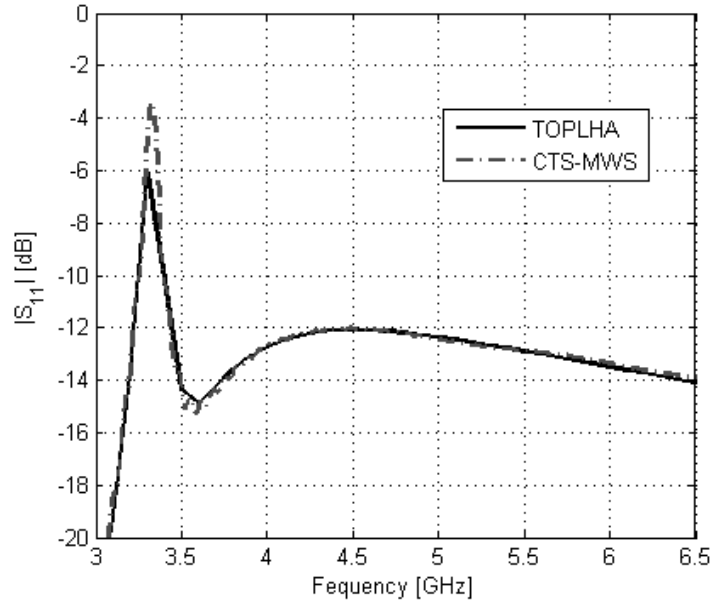

Figure 5. Plot of the magnitude (dB) of the reflection coefficient of the flanged rectangular waveguide, computed with TOPLHA (continuous line) and CTS-MWS (dashed-dotted line).

3.2. Waveguides with plasma

In recent years TOPLHA code has been carefully validated and benchmarked with several plasma codes, among which ALOHA (Advanced LOwer Hybrid Antenna) [9]
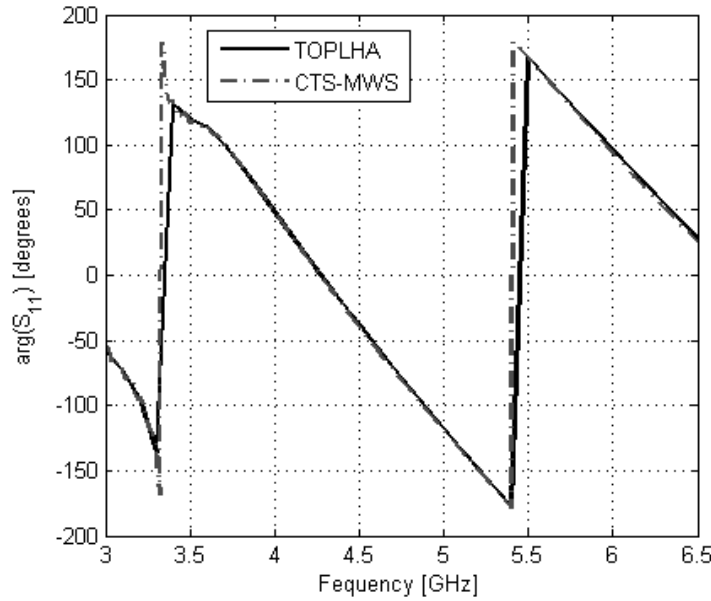
Figure 6. Plot of the phase (deg) of the reflection coefficient of the flanged rectangular waveguide, computed with TOPLHA (continuous line) and CTS-MWS (dashed-dotted line).

and GRILL3D [10], and against measured data in plasma-facing conditions for real-life structures [17]. Moreover, comparison of TOPLHA and the finite element software COMSOL has been carried out for a simple eight-waveguide grill geometry in [11]: the results are shown in Fig. 8 of mentioned reference.

To start with, an exhaustive comparison has been carried out with ALOHA code on the Tore Supra C2 antenna and, in the frame of EFDA task HCD-08-03-01, on a ITER-relevant PAM (Passive-Active Multi-junction) launcher; even though both validation campaigns are already part of published work ([9], [18]) we would like to provide here a short outline of the second comparison.

Specifically, the proposed 5 GHz launcher consists of 4 identical blocks of 12 rows of waveguides each, designed in order to deliver a maximum of 20 MW, and launching a power spectrum centered around $n_\parallel = 2$, being $n_\parallel = k_\parallel/k_0$. To simplify the codes comparison, the analysis has been limited to a single row, made up of 24 active waveguides (in dark color) and 25 passive waveguides (in light color), which dimensions are listed in Figure 7.

Passive waveguides are shorted after $\lambda_g/4$ from the mouth, λ_g being the guided wavelength at the operation frequency for the fundamental mode ; active waveguides have been connected to 6 multi-junction modules (as the one shown in Figure 8), which allow to obtain the required 270 degrees phasing at the antenna mouth. In both codes, the compound structure characterized by 6 reflection coefficients has been simulated by computing the scattering parameters of the open-ended waveguides (24x24 matrix after shortening the passive waveguides) and connecting that to the scattering matrix representation of the multi-junction module (1x4 matrix per module, as can be deduced
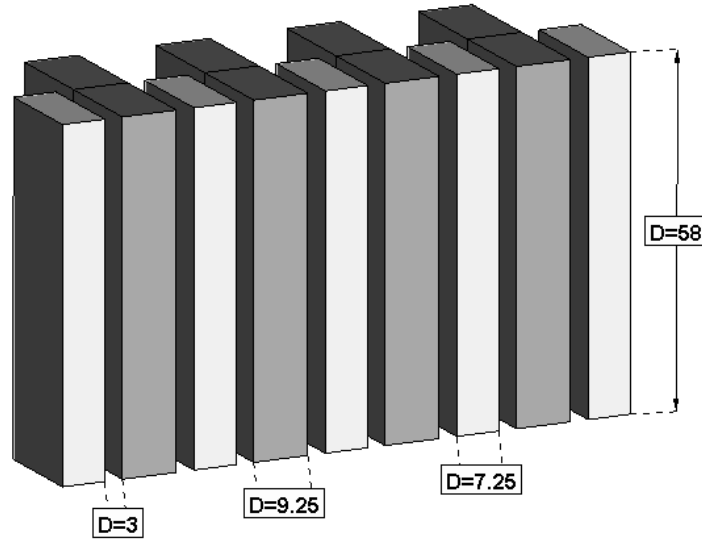
Figure 7. Portion of the simulated row of waveguides (in particular 4 active waveguides and 5 passive waveguide are shown) with its relevant dimensions (in mm).
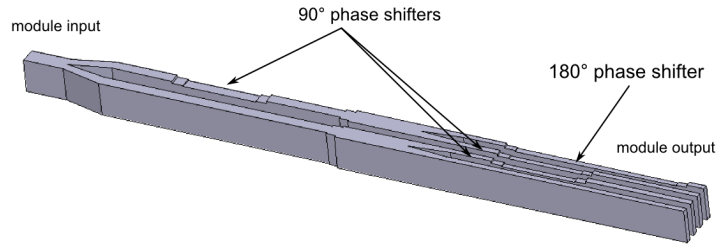

Figure 8. RF model of the 4-active and 4-passive multi-junction.

from Figure 8, see also [19]); the latter has been obtained by simulation with the commercial tool Ansoft HFSS †.

In terms of plasma description, a linear density profile in front of the antenna's mouth has been assumed: being x the radial direction, the profile has been computed as $n_e(x) = n_{e0} + \nabla n_e x$. To be precise, several edge densities n_{e0} have been taken into account, imposing two different density gradients (expressed using the scrape-off thickness $\lambda_{n0} = n_{e0}/\nabla n_e$) equal to $\lambda'_{n0} = 2mm$ and $\lambda''_{n0} = 2cm$ for each edge density.

The comparison has been first based on the reflection coefficient evaluated at the antenna mouth: imposing the expected phase at the mouth of the launcher (270 degrees), i.e. neglecting the multi-junction description, Figure 9 documents the average reflection coefficient $|\Gamma|^2$ (average among the 24 active waveguides simulated), defined as the ratio between backward and forward power.

The scattering matrix representation of the 6 multi-junction modules has been then connected to the active waveguides and the reflection coefficient has been determined at the input of each module; Figure 10 shows again the average reflection coefficient
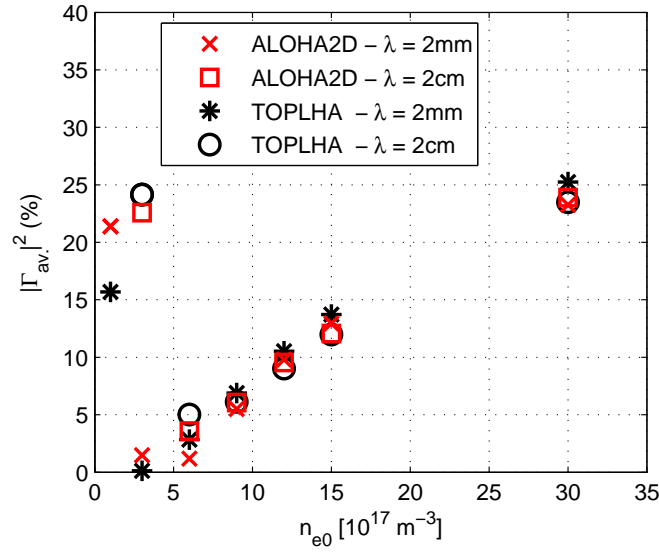
† www.ansoft.com/products/hf/hfss

Figure 9. Average reflection coefficient (in percentage) at the antenna's mouth, computed for different edge densities and two density gradients.
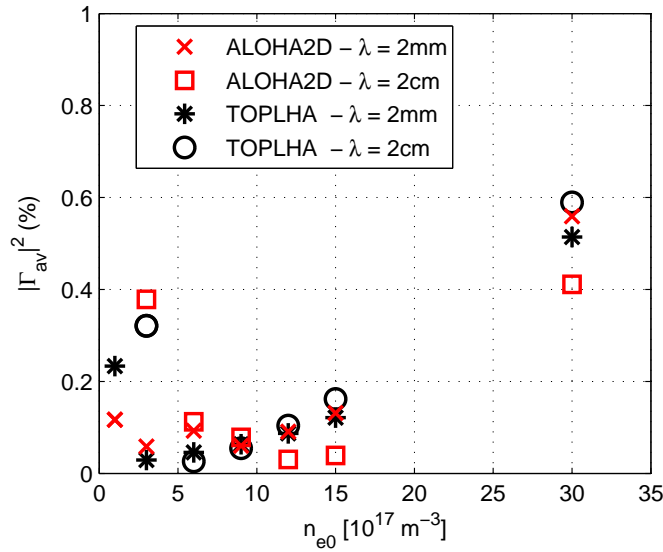

Figure 10. Average reflection coefficient (in percentage) at the beginning of the modules, computed for different edge densities and two density gradients.

(average among the 6 multi-junction modules) assuming that the modules are in phase.

Moreover, the power spectrum cut at $n_\perp = 0$ (where $n_\perp = k_\perp/k_0$) for a single $n_{e0} = 3 \cdot 10^{17} m^{-3}$ edge density has been evaluated with both density gradients and reported in Figures 11 and 12.

All the included pictures show a good agreement between the predictions of the involved simulation codes, providing a solid validation of TOPLHA code in presence of
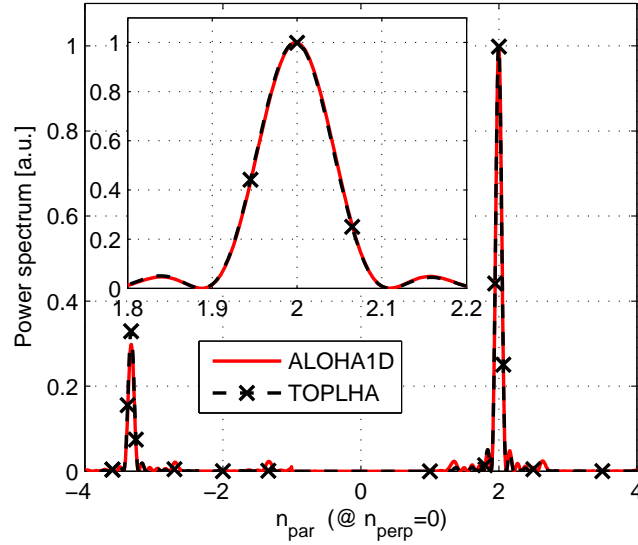
Figure 11. Cut of normalized power spectrum, at constant edge density $n_{e0} = 3 \cdot 10^{17} m^{-3}$ with $\lambda'_{n0} = 2mm$.
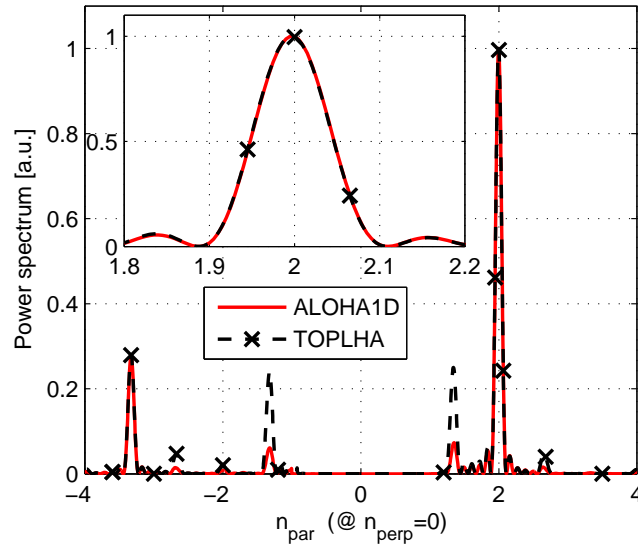

Figure 12. Cut of normalized power spectrum, at constant edge density $n_{e0} = 3 \cdot 10^{17} m^{-3}$ with $\lambda''_{n0} = 2cm$.

a real plasma loading. Concerning the computation time, TOPLHA code required for the reported analysis approximately 10 minutes on 400 cores at 2.3GHz of a Cray XT4 system.

Finally, to stress the main feature of TOPLHA code, i.e. the capability to handle any 3D geometry, a further comparison is documented: adopting 2 modules of the previously introduced ITER-relevant PAM launcher, a completely flat geometry is compared to a fully curved antenna (a small curvature is imposed both poloidally
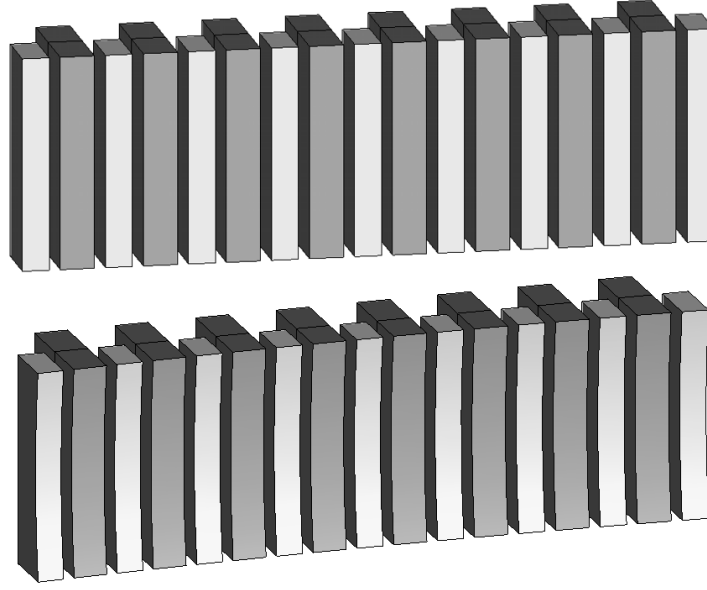
Figure 13. Simulated launcher (in particular 8 active waveguides and 9 passive waveguides are shown, same dimensions of Figure 7), in its flat (top) and curved (bottom) version.

and toroidally to comply with ITER torus dimensions), in terms of average reflection coefficient (average among the 2 multi-junction modules) and assuming that the modules are in phase. Figure 13 reports the two geometries, while Figure 14 and Figure 15 compare their performances in terms of the average reflection coefficients computed at the antenna's mouth and after the module insertion respectively. As the reader can notice, the introduction of the real curvature of the antenna front face has a not negligible impact on the computed results, above all when approaching the cut-off region.
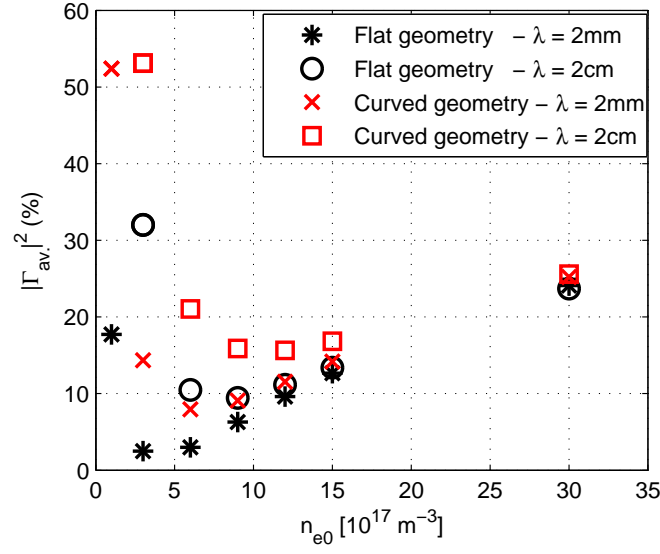
Figure 14. Average reflection coefficient (in percentage) at the antenna's mouth for the two simulated geometries, computed for different edge densities and two density gradients.
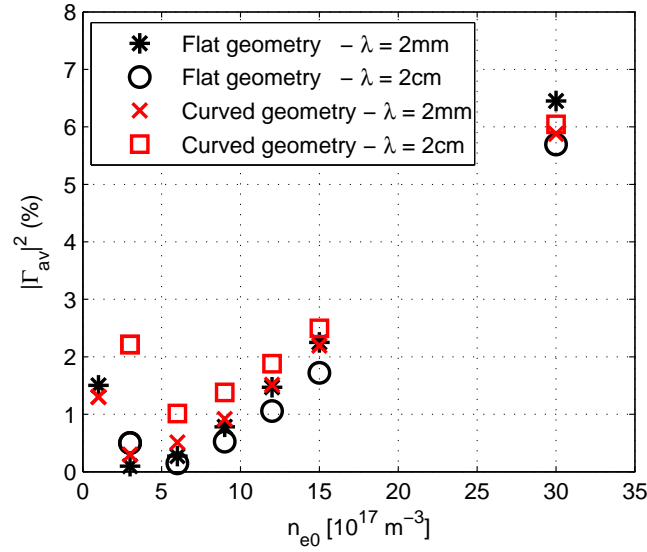

Figure 15. Average reflection coefficient (in percentage) at the beginning of the modules for the two simulated geometries, computed for different edge densities and two density gradients.

4. Conclusion and perspectives

This work has presented a detailed description of the theoretical advances recently introduced into TOPICA suite, giving rise to a new tool, TOPLHA. This code extends to Lower Hybrid launchers the well known capabilities of its predecessor, allowing the handling of realistic geometries with accurate plasma description. The confidence gained in the validation campaigns has then motivated the systematic use of TOPLHA in the actual design and optimization of LH antennas ([18]). Furthermore, TOPLHA code is fully parallelized, this leading not only to a remarkable saving in terms of computation time, but also to the removal of any limitation on the complexity of the simulated geometries and, specifically, on the number of waveguides.

Acknowledgments

References

[1] G.T. Hoang at Al.,"A lower hybrid current drive system for ITER ", *Nuclear Fusion*, vol. 49, 075001, 2009.

[2] V. Lancellotti, D. Milanesio, R. Maggiora, G. Vecchi, and V. Kyrytsya,"TOPICA: an accurate and efficient numerical tool for analysis and design of ICRH antennas", *Nuclear Fusion*, vol. 46, pp. S476–S499, 2006.

[3] D. Milanesio, O. Meneghini, V. Lancellotti, R. Maggiora, and G. Vecchi, "A multi-cavity approach for enhanced efficiency in TOPICA RF antenna code", *Nuclear Fusion*, vol. 49, 115019 (10pp), 2009.

[4] D. Milanesio, V. Lancellotti, L. Colas, R. Maggiora, G. Vecchi, and V. Kyrytsya, "Analysis of the Tore Supra ICRF antenna with TOPICA", *Plasma Physics and Controlled Fusion*, vol. 49, pp. 405–419, 2007.

[5] D. Milanesio, R. Maggiora, "ITER ICRF antenna analysis and optimization using the TOPICA code", *Nuclear Fusion*, vol. 50, 025007 (10pp), 2010.

[6] A. Messiaen, R. Koch, R.R. Weynants, P. Dumortier, F. Louche, R. Maggiora, and D. Milanesio, "Performance of the ITER ICRH system as expected from TOPICA and ANTITER II modelling", *Nuclear Fusion*, vol. 50, 025026 (21pp), 2010.

[7] A. Mendes, L. Colas, K. Vulliez, A. Ekedahl, A. Argouarch, and D. Milanesio, "Reduction of RF-sheaths potentials by compensation or suppression of parallel RF currents on ICRF antennas", *Nuclear Fusion*, vol. 50, 025021 (17pp), 2010.

[8] D. Milanesio, V. Lancellotti, O. Meneghini, R. Maggiora, G. Vecchi and R. Bilato "TOPLHA: an accurate and efficient numerical tool for analysis and design of LH antennas", in 17th Topical Conference on Radio Frequency Power in Plasmas, 2007.

[9] J. Hillairet, D. Voyer, A. Ekedahl, M. Goniche, M. Kazda, O. Meneghini, D. Milanesio and M. Preynas, "ALOHA: an Advanced LOwer Hybrid Antenna coupling code", *Nuclear Fusion*, vol. 50, 125010 (17pp), 2010.

[10] M.A. Irzak and O.N. Shcherbinin, "Theory of Waveguide Antennae for Plasma Heating and Current Drive", *Nuclear Fusion*, vol. 35, pp. 1341-1356, 1995.

[11] S. Shiraiwa, O. Meneghini, R. Parker, P. Bonoli, M. Garrett, M. C. Kaufman, J. C. Wright and S. Wukitch, "Plasma wave simulation based on a versatile finite element method solver", *Phys. Plasmas*, vol. 17, 056119 (10pp), 2010.

[12] R. Bilato and M. Brambilla, "Felhs code for lower-hybrid launcher coupling and near fields", in 35th EPS Plasma Physics Conf., page P5.094, 2008.

[13] M. Brambilla, "Modelling loop antennas for HF plasma heating in the ion cyclotron frequency range", *Plasma Physics and Controlled Fusion*, vol. 35, pp. 41–62, 1993.

[14] D.M. Pozar, *Microwave Engineering*, Wiley, New York, 1998.

[15] N. Marcuvitz, *Waveguide Handbook*, New York: McGraw-Hill, 1951.

[16] R.B. Marks and D.F. Williams "A General Waveguide Circuit Theory", *Journal of Research of the National Institute of Standards and Technology*, vol. 97, pp. 533–562, 1992.

[17] S. Ceccuzzi, R. Maggiora, D. Milanesio, F. Mirizzi and L. Panaccione, "Benchmark of Lower Hybrid coupling codes (Brambilla, GRILL3D-U, TOPLHA) with the FTU conventional grill experimental data", in 19th Topical Conference on Radio Frequency Power in Plasmas, 2011.

[18] D. Milanesio et Al., "Benchmark of coupling codes (ALOHA, TOPLHA and GRILL3D) with ITER-relevant Lower Hybrid antenna", *Fusion Engineering and Design*, vol. 86, pp.827-830, 2011

[19] J. Hillairet et Al., "RF modeling of the ITER-relevant lower hybrid antenna", *Fusion Engineering and Design*, vol. 86, pp.823-826, 2011